Available online at www.sciencedirect.com
SCIENCE DIRECT®
Polymer 45 (2004) 3359–3365
polymer
www.elsevier.com/locate/polymer

A flat polymeric gradient material: preparation, structure and property

Bianying Wen[a,*], Gang Wu[b], Jian Yu[a]

[a]Department of Chemical Engineering, Institute of Polymer Science and Engineering, Tsinghua University, Beijing 100084, People's Republic of China
[b]College of Materials Science and Engineering, Beijing University of Chemical Technology, Beijing 100029, People's Republic of China

Received 12 December 2003; received in revised form 26 February 2004; accepted 8 March 2004

Abstract

In this work, a novel processing method that combined extruding with laminate molding for preparing polymeric gradient material (PGM) has been investigated. Three modes of polypropylene/polyamide-6 flat PGM (signed with A1, A2, A3) are prepared successfully by using this new technique. The variation of composition, morphology and mechanical properties of specimens sampled along the thickness direction of these flat PGMs was confirmed and characterized through measurements of WAXD, elemental analysis, TEM observation and mechanical tests. Results indicate that the content of either polymer shows a gradient variation along the thickness direction. TEM photographs exhibit that morphology also evolves gradually with the varying percentage ratio of two polymers. As a result of such variations in composition and structure, the mechanical properties on both sides or from central part to outside of the flat PGMs exhibit a significant difference.

Keywords: Polymeric gradient materials; Preparation; PP/PA6 blend

1. Introduction

Functionally gradient materials (FGM) are inhomogeneous composites consisting of two or more components, which are designed such that their composition vary gradually in some spatial direction. Thus, FGM may take advantage of certain desirable features of each of the components, and this makes it more suitable to match the needs of working environment than that of homogeneous composite. So it attracted more scientists' attention since it is proposed. In the past years, a lot of work was done in the field of FGM, especially for their application as thermal barrier material [1–4]. Many ways of fabricating FGMs have been developed, such as powder processing, thermal spraying, chemical vapor deposition, physical vapor deposition, combustion synthesis, diffusion treatment and so on [5–8]. In recent years, the concept of FGM is extended to other research field, such as photoelectric, thermoelectric, and nuclear energy conversion materials [9, 10]. It is a pity that those works focussed more on the lower molecular weight substances like ceramic, metal and other inorganic materials but only few experimental studies focussed on polymeric gradient materials (PGM). After 1990s, several researchers published their fabricating methods or ideas on the preparation of PGM. These methods include dissolution diffusion, cast, emulsion-blend, and coating; fibers stacked gradually up in a matrix, degradation under UV light and other ways [11–15]. In many of the above-mentioned methods, however, fabrication costs may be high-priced because of the specialized equipment used. In addition, product size is restricted due to the complex processing techniques involved. The aim of this study, therefore, is to try to devise a simple, inexpensive and repeatable way to prepare PGM by use of conventional polymer processing facilities. This paper describes a novel method that combined extruding with laminate molding for preparing PGM, and three modes of polypropylene (PP)/polyamide-6 (PA6) flat PGM (signed with A1, A2, A3) are prepared successfully by using this new technique.

In all of the following, mode A1 will be discussed particularly; the other two being used as reference materials for comparison.

* Corresponding author. Tel.: 86-10-62781495; fax: 86-10-62770304.
E-mail address: wby@mail.tsinghua.edu.cn (B. Wen).

0032-3861/$ - see front matter © 2004 Elsevier Ltd. All rights reserved.
doi:10.1016/j.polymer.2004.03.023

2. Experimental

2.1. Materials

Commercial polypropylene (PP) and polyamide-6 (PA6) pellets used in this study were kindly provided by Qilu Petrochemical Inc. and Yueyang Chemical Plant, respectively. The melt flow index (MFI) of PP as measured at 230 °C and 2.16 kg is 4. MFI measured at 245 °C and 2.16 kg for PA6 is 12. PP-*g*-MAH pellets, as a compatibilizer in this system, are prepared using melting graft technique in our lab.

2.2. Sample preparation

A schematic diagram of the processing route for preparing flat PGMs is shown in Fig. 1. A Prism TSE-16-TC twin-screw extruder with a screw diameter of 16 mm and a length to diameter ratio of 25 was used to melt and extrude the blend. An extrusion die with a rectangular slot having a size of 18 mm × 1 mm was assembled. In order to prepare the PGMs, physical mixing of the components was carried out prior to the melt extruding process. A feedstock series in which the weight ratio of the components varied gradually was designed. Such a feedstock series is fed in the extruder as a function of processing time. The resulting extrudate with continuously varying weight fraction of the components was obtained after being blended and extruded. For this experiment, as the hatching shows in Fig. 2, PP, PA6 and PP-*g*-MAH were mixed with different weight ratio, i.e. (PP + PP-*g*-MAH)/PA6 = 100/0, 90/10, 80/20, 70/30, 60/40, 50/50, 40/60, 30/70, 20/80, 10/90, and 0/100, and the ratio of PP-*g*-MAH also varied in this feedstock, as the folding line with symbols has shown in the same figure. Such a feedstock series in which PA6 is gradually increased is fed in extruder one by one in every 0.5 min interval. The rotating speed 50 rpm of screws and melt blending temperature of 215–260 °C was used. The PP/PA6 blended strip with gradually varied weight fraction was molded through the rectangular extrusion die. Such a strip was cooled firstly, and was cut into a series of segments with certain length for collocated. In mode A1, the segments were arrayed in a sequence in which the content of PA6 increased from one side to another side along its thickness direction; in mode A2 and A3, the segments were arrayed symmetrically in such sequence in which the content of PA6 decreased or increased from the central part to the outside, respectively. Same layers (or segments) were employed in all of the three modes of PGMs. Finally, the rough products were laminated molding using a curing press (50t), separately. The laminated molding parameters are shown in Table 1.

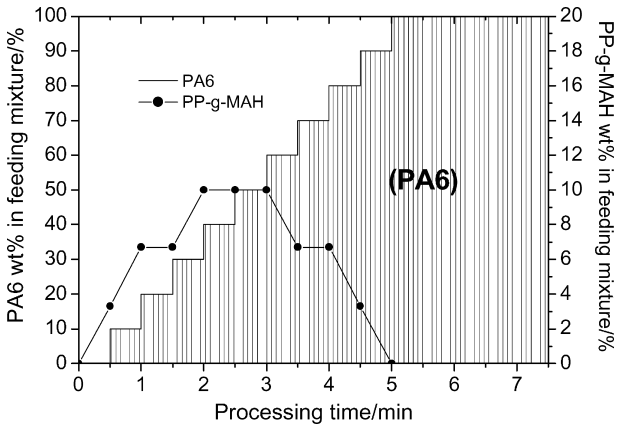

Fig. 2. The relationship between weight percentage of PA6 or PP-*g*-MAH in feeding mixture and processing time.

Obviously, the gradient that exists in the PGM can be controlled conveniently by changing the feeding speed and/or weight ratio of the components. In addition, the thickness of the flat PGM can be controlled easily through the change of the numbers of the folded layers.

2.3. Characterization

Fig. 3 shows a schematic diagram for testing specimens sampled from a flat PP/PA6 gradient material (mode A1). The thickness of the PGM is about 4 mm. As shown in Fig. 3, the sample could be sliced to seven parts along the thickness direction, and which be sighed with S1,S2,…,S7, respectively. Such seven specimens were used for X-ray diffraction, elemental analysis, TEM observation and mechanical tests.

2.3.1. X-ray diffraction

Wide-angle X-ray diffraction (WAXD) measurements were carried out on a Shimadzu XRD-6000 diffractometer

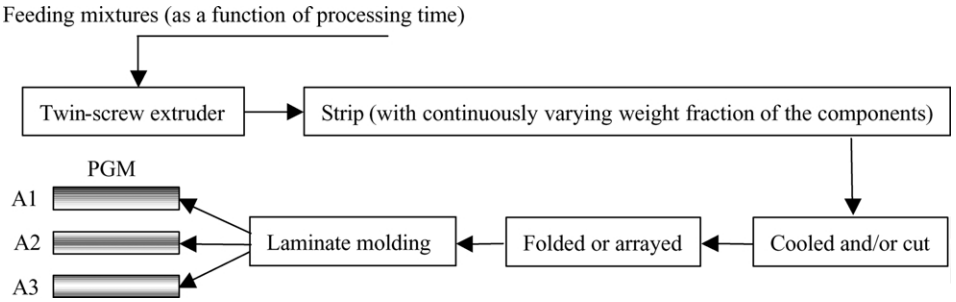

Fig. 1. The schematic diagram of the processing route for preparing flat PGM.

Table 1
Laminate molding parameters

PP/PA6 PGMs	Molding board temperature (°C)		Pressure (MPa)	Time (min)
	Upside	Underside		
A1	220	160	4–5	50
A2	215	215	4–5	15
A3	220	220	4–5	30

system with Cu K_α radiation generated at 40 kV and 30 mA. The diffracting intensities were recorded for every 0.02° from 2θ scan in the range of 5–40° at a scanning speed of 5 °/min.

2.3.2. Elemental analysis

A Carlo Brba 1106 elemental analyzer was used to determine the content of PA6 in PP/PA6 blend through measuring the weight percentage of the nitrogen element in the corresponding samples. The weight of each sample was about 1 mg.

2.3.3. Morphology observations

Morphological variation of the PP/PA6 gradient materials was studied using a Hitachi-800 transmission electron microscope. Samples were sliced at liquid nitrogen temperature. The ultrathin sections were dyed by RuO_4 for taking micrographs.

2.3.4. Mechanical property test

The mechanical properties of the specimens were measured on an Instron 1185 tester at room temperature. All experiments including tensile and bending tests were performed with a constant crosshead speed of 10 mm/min.

3. Results and discussions

3.1. Gradient variation of composition

In order to study the gradient variation of composition and obtain some information that concerned with their crystallization, analysis was first performed on specimens S1 to S7 with X-ray diffraction measurement. The intensities of X-ray diffraction versus 2θ angle for these specimens are shown in Fig. 4. Besides, to be compared

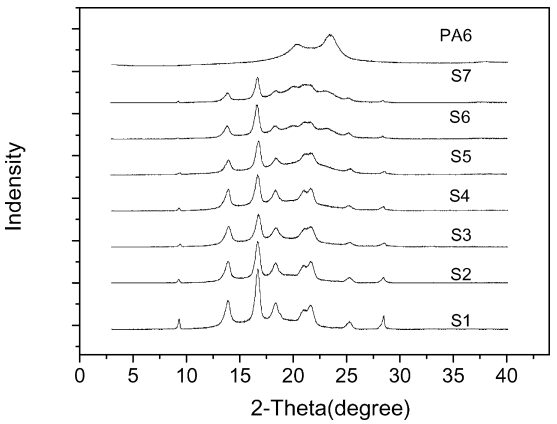

Fig. 4. X-ray diffraction profiles of specimens as a function of diffraction angle.

with the blend, pure PA6 also be measured together. As shown in Fig. 4, the curve of specimen S1 (at the bottom of the figure) reveals several diffraction peaks at ca. $2\theta = 13.8$, 16.7, 18.4, 21.0 and 25.3°, which may be assigned to (110), (040), (130), ($13\bar{1}$) and (150) reflection of the α form crystals of PP. The absence of other peaks indicates that specimen S1 consists of pure PP [16,17]. The intensity curve of pure PA6, as seen at the top of the figure, shows two diffraction peaks at ca. $2\theta = 20.3$ and 23.4°, which are attributed to the α(100) and α(002)/(202) crystal planes of PA6 [18–20], respectively. By comparison with WAXD scans of two such extreme cases, WAXD curve of other specimens, i.e. S2 to S7, seems to be a combination of pure PP and PA6. In other words, respective characteristic peaks from PP and PA6 appear synchronously in six such traces, although the peak of PP and PA6 overlap in the vicinity of $2\theta = 20$–21°. This is an evident indication of coexistence of two substances. The relative intensity of respective peaks changes gradually with varied sampling position. For example, the strongest (040) reflection of PP becomes weaker and weaker, while the (002) peak of the PA6 becomes stronger and stronger from S1 to S7. The diffraction intensity is considered to be a direct reflection of the percentage variation of specific substances. Such a systematical decrease or increase in both diffraction peaks of PP and PA6 indicates that the relative content of PP and PA6 varied gradually along the thickness direction. Besides, because no other new diffraction peaks occurred in six such traces, the results suggest that no other new crystal structure formed in the blend.

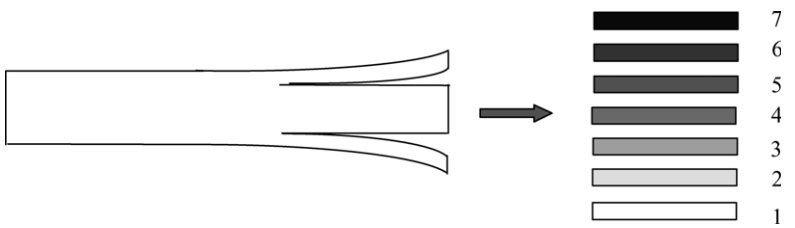

Fig. 3. The schematic diagram of the specimens sampled from a flat PGM.

It is well known that the value of the diffracted intensity is directly proportional to the crystallinity in a homopolymer material. This value, however, cannot be used to evaluate the content of either polymer in a bicomponent blend. In other words, the quantitative weight percentage of either PP or PA6 in each specimen cannot be determined with current WAXD data. For clarifying the point at issue, elemental analysis is considered to be a useful tool. Since the nitrogen (N) element only exists in the PA6 component in the whole experimental system, after the content of nitrogen element in blend being determined, the weight percentage of PA6 in the corresponding specimen can be calculated [21,22].

Following equation was used to calculate the weight percentage of PA6 (PA6%) in various PP/PA6 blended specimens,

$$\mathrm{PA6\%} = (M_0/M_\mathrm{N})N\%$$

where M_0 is the repeat unit chemical formula weight of the PA6, M_N is the atomic weight of nitrogen element, and $N\%$ is the percentage of nitrogen in blends which is determined by elemental analysis. The calculated results for specimens 1–7 are shown in Fig. 5. It shows that the content of PA6 increases gradually from one side to another side along the thickness direction in mode A1, and decreases or increases gradually from central part to the outside in mode A2 and A3, respectively. As designed, A2 and A3 show the symmetric feature while A1 is asymmetric.

3.2. Evolution of morphology

The morphology for the PP/PA6 PGM was examined by transmission electron microscopy. Typical TEM photographs of the PP/PA6 gradient materials sampled at different positions along the thickness of mode A1 are presented in Fig. 6(a)–(f). Because the sliced PP/PA6 specimens were undergone a pre-treatment in which the component PA6 was dyed by RuO_4, as seen in these photographs, therefore, the white area and black one represent the PP and PA6 phase, respectively. As determined by WAXD and elemental analysis, S1 consist of pure PP, no more morphological information is observed, so it is not listed in this figure. Following four kinds of morphological feature appear in Fig. 6. (1) PA6 particles disperse in PP matrix and results a so-called 'sea-island' morphology. This morphological structure exists in Fig. 6(a)–(c), corresponding to S2, S3 and S4 in which the percentage of PA6 is lower than 30%. So PA6 forms 'islands' while PP forms the 'sea'. Comparing these three pictures, it is evident that the numbers of the 'islands' increase gradually from (a) to (c). This attributed to that the increase of PA6 content from S2 to S4 (see Fig. 5). (2) PA6 ribbons penetrate in PP and forms interpenetrated morphology. In general, when the ratio of components in a bicomponent blend is nearly symmetrical, it often forms co-continuous interpenetrate morphology, according to traditional blended systems [23–26]. Because the percentage of PA6 in S5 has reached to 47%, which is close to that of PP, the morphology of S5 is PA6 ribbons penetrate through PP matrix, although the ribbons in Fig. 6(d) looked like particles apparently due to the direction of taking photos perpendicular to that of ribbons longness. This fact has been confirmed in a SEM observation, in which some columnar cavities are identified after etching the PA6 phase, for more details refer to our previous published work [27]. The interpenetrated morphology is an intergradation of PA6 from dispersed phase to continuous phase and means a phenomenon of phase inversion begin to occur. (3) PP and PA6 forms a co-continuous sandwich-like morphology, as shown in Fig. 6(e). Because the percentage of PA6 is dominant (about 65%) in S6, it is found that the thickness of PA6 layer is thicker than that of PP layer. It is also found that PA6 or PP particles dispersed in their opposite phases, together, indicate that a 'dual mode' of dispersed morphology is formed in the sandwich zone. (4) PP particles dispersed in PA6 matrix as shown in the last picture of Fig. 6. In this region, the content of PA6 closed to 80%, so PP forms 'islands' while PA6 forms the 'sea'. This means the phase inversion has accomplished. By careful observation in Fig. 6(e) and (f), it is found that an opposite component diffused in some PP or PA6 droplet, this means that the compatibility between the PP and PA6 has improved by added with PP-*g*-MAH.

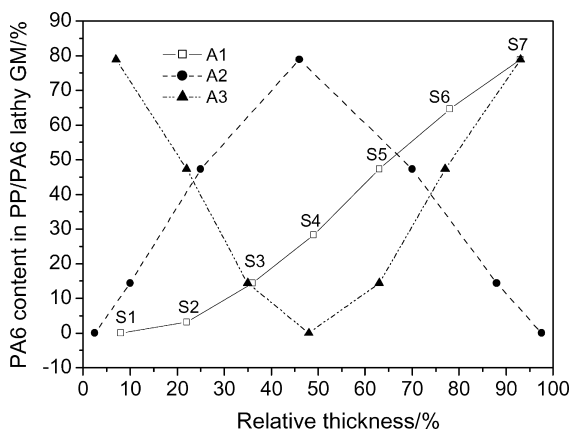

Fig. 5. The variation of PA6 wt% in flat PP/PA6 PGMs along the thickness direction.

Above observations indicate that the dispersed phase morphology forms when either polymer is in a lower level, and a co-continuous morphological structure forms when the content of PA6 is increased to be close to that of PP. A phase inversion phenomenon appears when the content of PA6 is higher than that of PP. The morphological feature of respective specimen is similar to the traditional blend in which the difference between any two domains could be neglected. The whole structure of the PGM prepared in this study, however, is very different from the traditional blend because the morphology of each sliced specimen varies gradually along the thickness direction of the flat PGM.

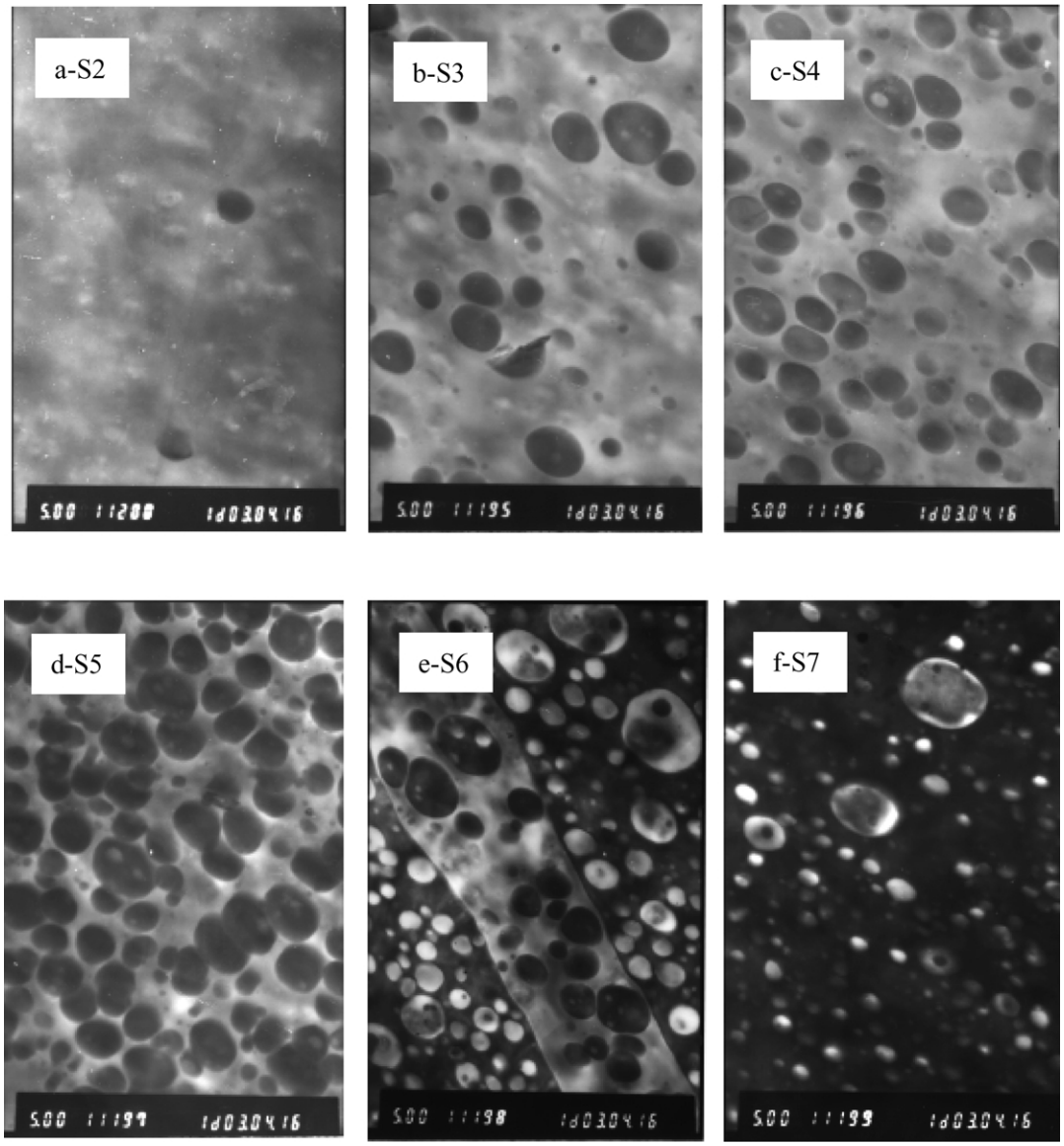

Fig. 6. TEM photographs of specimens sampled at different positions in flat PP/PA6 PGM.

These results indicate clearly that the gradient structure has been formed in the material.

3.3. Mechanical properties

3.3.1. Tensile properties

It is well known that the performance of a blend is affected intensively by its composition and morphological structure. Figs. 7–9 show the variation of tensile strength, Young's modulus and elongation at break of three modes of flat PGMs along the thickness direction. In the case of S1, the tensile strength of about 24 MPa, the Young's modulus of 380 MPa and the elongation at break of about 1300% are typical values for pure PP. With the increase in content of PA6, the elongation value exhibits a decline tendency while Young's modulus increased monotonously. In contrast with that, tensile strength shows diverse variation, which appears

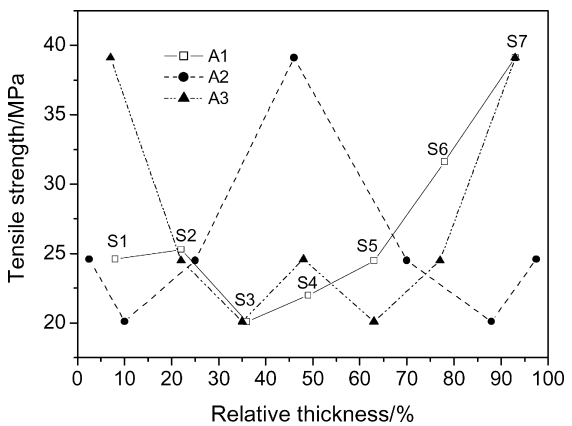

Fig. 7. The variation of tensile strength in flat PP/PA6 PGMs along thickness direction.

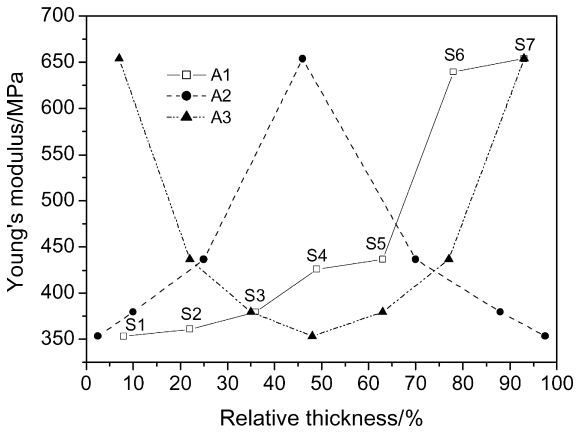

Fig. 8. The variation of Young's modulus in flat PP/PA6 PGMs along thickness direction.

more affected by the weight ratio of the components and morphological structure of the blend.

It is shown that adding a little of PA6 has a positive effect in improving the mechanical property of the PP. For example, the tensile strength, Young's modulus and elongation at break increased synchronously in S2 in which the content of PA6 is only 3%. Higher than that, the tensile properties except Young's modulus decreased significantly. In the range of PA6 content from ca. 14 to 47%, which corresponds to three of the specimens, i.e. S3, S4 and S5 (see Fig. 5), the tensile properties show a worst level due to the increase of particle size of dispersion phase and poor interfacial adhesion. A dramatic change in the Young's modulus and other two tensile properties take place from S5 to S6. It is observed that all of the values of the three tensile properties increased significantly. The reason for which is the formation of co-continuous morphological structure (see Fig. 6(e)). This benefits the dispersion and transfer of the stress. When the phase inversion finished, as shown in S7, tensile properties except elongation also increased. Experimental facts indicate that the properties of a blend depend more on the component with continuous phase as well as the morphology of the blend.

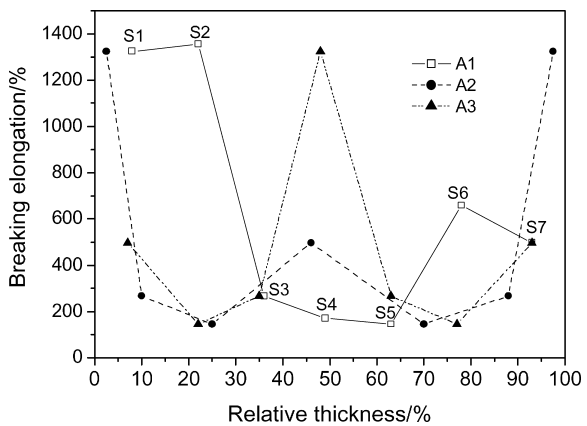

Fig. 9. The variation of elongation at break in flat PP/PA6 PGMs along thickness direction.

3.3.2. Bending property

Above tensile test determined the property of separated part of the flat PGM, which reflect the variation of mechanical property along the thickness direction while the whole property of the flat PGM is not reflected. As a complementarily, bending test on whole flat PGMs was performed [28]. Because A1 belongs to asymmetric material, bending tests on A1 were performed in two opposite directions. All bending stress–strain curves of the three modes of flat PGM are shown in Fig. 10, and the corresponding determined results are listed in Table 2. Results indicate that, A3 has the highest bending strength and bending modulus, which is nearer to that of pure PA6; this is attribute to the higher content of PA6 (about 80%) on its two sides. Although PP is rich on its two sides of A2, due to PA6 is rich in its middle part, the bending strength is higher than that of pure PP. The difference between curve A1-1 (bended towards the side near which PP is rich) and A1-2 (bended towards the side near which PA6 is rich) is obvious. A1-2 is better than A1-1 in bending resistance. So A1 or asymmetric PGM may suit to the situation where the special bending is required.

4. Conclusions

On investigating the variation of composition, structure and property of three modes of the flat PGMs, it is concluded that the composition, structure and the mechanical property varied gradually among the inside of the materials on a certain direction which is predesigned. The morphological feature of respectively sliced specimen from the PGM is similar to the traditional blend in which the difference between any two domains could be neglected. The whole structure of the PGM prepared in this study, however, is very different from the traditional blend because the morphology varies gradually along its thickness direction of the materials. The mechanical properties of the PGMs depend directly on the weight ratio of components and morphological structure, and show divers

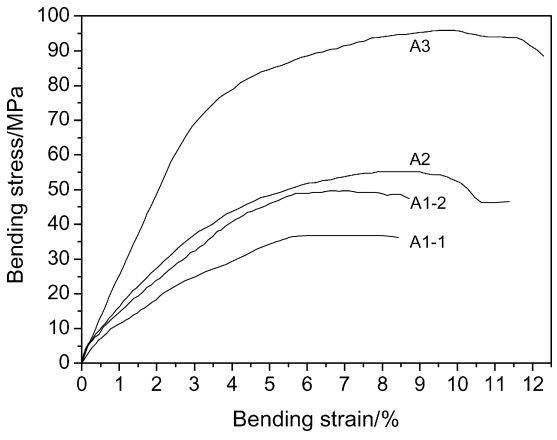

Fig. 10. Bending stress–strain curves of PP/PA6 flat PGMs.

Table 2
Bending properties

Materials	Bending strength (MPa)	Bending modulus (MPa)
A1-1 (bended towards the side near which PP is rich)	37.6	1210
A1-2 (bended towards the side near which PA6 is rich)	50.1	1466
A2	55.7	1319
A3	96.2	2405
Pure PA6	98.0	2452
Pure PP	48.3	1373

result. More studies need to be done in improving the property of the materials. All experimental results show that the PP/PA6 flat gradient material can be prepared successfully by the use of this special extruding laminate molding technique.

Acknowledgements

The support from Natural Science Foundation of Beijing City (grant No. 2012014) was gratefully appreciated.

References

[1] Koizumi M. Composites: Part B 1997;28:1.
[2] Markworth AJ, Ramesh KS, Parksjr WP. J Mater Sci 1995;30:2183.
[3] Jackson TR, Liu H, Patrikalakis NM, Sachs EM, Cima MJ. Mater Des 1999;20:63.
[4] Hui PM, Zhang X, Markworth AJ, Stroud D. J Mater Sci 1999;34:5497.
[5] Ma J, Tan GEB. J Mater Process Technol 2001;113:446.
[6] Laux T, Killinger A, Auweter KM, Gadow R, Wilhelmi H. Mater Sci Forum 1999;308–311:428.
[7] Kawasaki A, Watanabe R. Engng Fract Mech 2002;69:1713.
[8] Liu GR, Han X, Lam KY. J Compos Mater 2001;35:954.
[9] Kaysser WA. Mater Sci Forum 1999;308–311:1068.
[10] Uemura S. Mater Sci Forum 2003;423–425:1.
[11] Kano Y, Akiyama S, Sano H, Yui H. Polym J 1997;29:158.
[12] Agari Y, Shimada M, Ueda A, Nagai S. Macromol Chem Phys 1996;197:2017.
[13] Chekanov YA, Pojman JA. J Appl Polym Sci 2000;78:2398.
[14] Jang J, Han S. Composites: Part A 1999;30:1045.
[15] Lambros J, Santare MH, Li H, Sapna III GH. Exp Mech 1999;39:184.
[16] Assouline E, Grigull S, Marom G, Wachtel E, Wagner HD. J Polym Sci: Part B 2001;39:2016.
[17] Homsby PR, Tung JF. Plastics Rubber Compos Process Appl 1995;24:69.
[18] Liu TX, Liu ZH, Ma KX, Shen L, Zeng KY, He CB. Compos Sci Technol 2003;63:331.
[19] Campoy I, Gomez MA, Macro C. Polymer 1998;39:6279.
[20] Liu XH, Wu QJ. Eur Polym J 2002;38:1383.
[21] Niyogi S, Maiti S, Adhikari B. Polym Engng Sci 2002;42:336.
[22] Thamizharasi S, Reddy BSR. J Appl Polym Sci 2001;80:1870.
[23] Wilkinson AN, Laugel L, Clemens ML, Harding VM, Marin M. Polymer 1999;40:4971.
[24] Tseng FP, Lin JJ, Tseng CR, Chang FC. Polymer 2001;42:713.
[25] Bertil O, Hassander H, Tomell B. Polymer 1998;39:4715.
[26] Roeder J, Oliveira RVB, Goncalves MC, Soldi V, Pires ATN. Polym Test 2002;21:815.
[27] Wen BY, Li QC, Hou SH, Wu G. Mater Sci Forum 2003;423–425:509.
[28] Nunes JP, Pouzada AS, Bernardo CA. Polym Test 2002;21:27.